

A proton T_1 -nuclear magnetic resonance dispersion study of water motion in snowflakes and hexagonal ice

Per-Olof Westlund

To cite this article: Per-Olof Westlund (2019) A proton T_1 -nuclear magnetic resonance dispersion study of water motion in snowflakes and hexagonal ice, *Molecular Physics*, 117:7-8, 960-967, DOI: 10.1080/00268976.2018.1541197

To link to this article: <https://doi.org/10.1080/00268976.2018.1541197>



© 2018 The Author(s). Published by Informa UK Limited, trading as Taylor & Francis Group



Published online: 30 Oct 2018.



Submit your article to this journal [↗](#)



Article views: 628



View related articles [↗](#)



View Crossmark data [↗](#)

A proton T_1 -nuclear magnetic resonance dispersion study of water motion in snowflakes and hexagonal ice

Per-Olof Westlund 

Department of Chemistry: Theoretical and Computational Chemistry, Umeå University, UMEÅ, Sweden

ABSTRACT

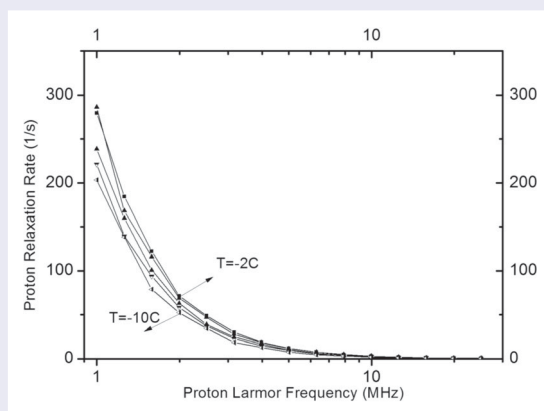
Snowflakes and ordinary hexagonal ice were studied measuring water proton spin–lattice relaxation rate $R_1(\omega_l)$ -nuclear magnetic resonance dispersion (NMRD) profiles at proton Larmor frequencies ranging from 1 to 30 MHz and at different temperatures ranging from -2°C to -10°C . The spin–spin relaxation rate $1/T_2(\omega_l)$ was determined at a single Larmor frequency of 16.3 MHz. The high-field wing of the proton $R_1(\omega_l)$ -NMRD profile was characterised by two parameters: a correlation time τ_c which described the dipole–dipole spectral density, and the relaxation rate at low fields $R_{\text{real}}^{\text{max}}(0)$ which was determined from T_2 . The correlation time τ_c depended on the dynamic model used. A rotation diffusion model yield approximately $3 \mu\text{s}$ at -3°C to about $5 \mu\text{s}$ at -10°C , whereas for a more realistic six-site discrete exchange model, the correlation times decreased slightly to about 80% for the same temperature interval. Proton dipole–dipole interactions were divided into intramolecular and intermolecular contributions where the intermolecular contribution was about $0.4\text{--}0.8 \times$ the intramolecular contribution. It was not possible to discriminate between the dynamic models or to detect ice/water interface effects by comparing the NMRD data from snowflakes with ordinary hexagonal ice data.

ARTICLE HISTORY

Received 20 June 2018
Accepted 12 October 2018

KEYWORDS



Six-site exchange model;
water dynamics in hexagonal
ice; water proton spin–lattice
relaxation dispersion



1. Introduction

The water molecular structure and motions in hexagonal ice were first studied almost 70 years ago [1–11]. Over 50 years ago, a *Nuclear magnetic resonance (NMR)* relaxation study was reported by Barnaal and Lowe [1] in which they used high-purity single crystals of ice to search for an orientation-dependent T_1 relaxation time. Their analysis was based on the Bloch–Wangsness–Redfield (BWR) perturbation theory [9] in combination with a discrete exchange model for the reorientation dynamics

of the water proton dipole–dipole interaction. A single activation energy (59 kJ/mol) for the T_1 process was determined for temperatures ranging from $T = 0$ to -60°C . From spin–lattice relaxation times measured at a proton Larmor frequency of 10 MHz, they derived the relation $T_1 = C(\omega_0)\tau_c$ between the proton spin–lattice relaxation time T_1 and the correlation time τ_c describing the fluctuation of the proton dipole–dipole interaction. The numerical factor $C(10\text{MHz}) = 2.14 \times 10^5$ (see Equation (9)) was based on their discrete exchange model

CONTACT Per-Olof Westlund  per-olof.westlund@umu.se  Department of Chemistry: Theoretical and Computational Chemistry, Umeå University, 901 87 UMEÅ, Sweden

where water molecules were allowed to move between six different configurations with equal probability as a result of lattice defects (Bjerrum fault migration) and in accordance with the Bernal–Fowler ice rules [2]. From this work, it is clear that proton spin–lattice relaxation in hexagonal ice is taking place under *slow reorientational conditions*, $\omega_I \tau_c \gg 1$. The importance of the intramolecular dipole–dipole interaction was estimated to about 56% of the total second moment [1]. The correlation time at -3°C ($\tau_c = 2.5 \mu\text{s}$) and, $5.5 \mu\text{s}$ at -10°C was considerably shorter than the correlation time obtained from dielectric relaxation. The nominal length of their FID was $15 - 30 \mu\text{s}$ and no anisotropy for T_1 could be detected [1].

Onsager and Runnels [3] also investigated the relaxation phenomena in ice and compared elastic relaxation with dielectric relaxation and proton NMR T_1 measurements. The water dynamics model used was based on the migration of Bjerrum defects among six possible orientations with the same probability. When a defect occurs, the water molecules can reorient into four different orientations with equal probability. BWR relaxation theory was used to relate the water dynamics to the NMR spin–lattice relaxation time T_1 . It was pointed out that the proton dynamics was an order of magnitude faster compared to estimation using dielectric relaxation [3].

Weihause et al. [4] measured the rotating frame $T_{1\rho}$ and T_1 at 28 MHz and reported a correlation time of τ_c (-10°C) = $6.9 \mu\text{s}$. Bruno and Pintar [5] estimated the correlation time to be $3.8 \pm 1 \mu\text{s}$ at -24°C . They concluded that ‘it is not possible to differentiate between different models since T_{1D} and τ_c are known with little precision’. However, Geil et al. [6] focused on investigating the details of the dynamic processes of protons in ice. Heavy water was used to study the slow proton motion in hexagonal ice. A fast motion correlation time ($\tau_c^{(f)}$) which is relevant to the present work was estimated as $1.8 - 3 \mu\text{s}$ for the temperature interval -3°C to -10°C as shown in their Figure 11 and in Equations (2) and (A3). In [7], the ^1H spin–lattice relaxation in ice was considered to be due to modulation of the dipole–dipole interactions from a molecular diffusion via an interstitial process. Gran et al. [8] studied water dynamics in doped hexagonal ice using proton T_1 NMR relaxation data at one Larmor frequency. They noted that the ^1H -spectrum consisted of a small narrow peak superposed on a broader peak. Interestingly, the study included pure and doped ice and natural snow where the temperature variation of the ^1H -NMR spectrum (at 60 MHz) and T_1 (at 8 MHz) were measured. One aim was to find a surface-to-volume dependence of the ^1H -spectrum by comparing snowflakes and ordinary ice. However, no such dependence was detected. The

Gaussian line-shape at low temperatures became more Lorentzian above -6°C . The correlation times reported for pure ice (their Figure 7) τ_c were large ranging from 9 to $25 \mu\text{s}$ for $T = 0^\circ\text{C}$ to -10°C [8]. Similarly to ref [1], a relation was found between T_1 and the effective correlation time τ_c reading $T_1 = 4.74 \times 10^4 \tau_c$ with a numerical factor C which is about 35% of the value of Barnaal and Lowe indicating a much larger fraction of the intermolecular dipole–dipole contribution.

It is difficult to extract detailed information about the actual water dynamic model in ice from T_1 measurements alone [3, 5]. Different dynamic models give different ranges of correlation times for equally high-quality fits to the experimental data. In particular, the discrete six-site exchange model gives shorter correlation times compared to a simple isotropic diffusion model.

In the present work, we demonstrate how a *relatively limited* proton T_1 -Nuclear Magnetic Resonance Dispersion (NMRD) profile can be used to estimate the fast motion of water in hexagonal ice for a temperature interval from -2°C to -10°C . The analyses of the high-field wing of the T_1 -NMRD profile uses the spin–spin relaxation rate measurements at one single field assuming $T_2 = T_2^*$.

We also investigate *whether* it was possible to detect a relaxation effect due to the surface-to-volume difference between hexagonal ice and snowflakes using proton relaxation measurements. However, the results were complicated by imprecise temperature measurement of the sample. This was due to a combination of sample size and how the temperature was measurement indirectly from the flow of air before it hit the sample. The instrument construction made it difficult to avoid a large temperature gradient in the sample.

2. Experiment and sample

Snowflakes were collected in January 2015 and 2017 in the late evening during a couple of days of snowfall in Umeå at the temperature of approximately -15°C to -20°C and then packed directly into 10 mm NMR tubes. The 2015 samples were 1.4 ml, whereas the 2017 samples were 0.5 ml. The ice samples were obtained by melting ice-flake samples and then freezing to form ordinary hexagonal ice. The 10 mm NMR tubes for NMRD study were sealed and kept at a temperature of -20°C . The formation of ice-flakes is not a controllable process but is expected to depend on the purity of the air within which they are formed. However, the reproducibility of T_1 values of the snowflake and ice samples collected at different occasions was excellent.

2.1. Proton 1H T_1 and T_2 relaxation measurements

The proton longitudinal relaxation rate, $R_1^{\text{exp}}(\omega, T)$ was measured on a 1T Stellar FFC2000 fast field cycling instrument with polarisation at 25 MHz and detection at 16.29 MHz. The spin–lattice relaxation takes place at proton Larmor frequencies ranging from 0.01 to 40 MHz, however, it was only possible to detect a signal for Larmor frequencies larger than 1 MHz when $T_1 \geq 3$ ms. The experimental data of the 2017 sample are presented in Figure 1. Spin–spin relaxation was detected at one Larmor frequency (16.29 MHz) and was obtained by averaging the spin–spin relaxation time over several zones of the data file. The values of T_2^* was about 7–12 μs . Consequently, the contribution from inhomogeneous broadening was considered negligible and a proper spin-echo experiment was not possible because of the very short T_2 . We thus assume $T_2^* = T_2$. The switching time was 3 ms, and a 90°C pulse length of 8.1 μs were used. The polarisation and recovery time were set to $4 T_1$ and the number of accumulated transients was 4 for all samples. The sample temperature was 263–270 K, determined within $\pm 0.7^\circ$ which was checked by measuring the temperature in a water sample at different temperatures according to the spectrometer. Generally, the sample temperature was 0.5 – 0.8° higher according to an external thermometer. The maintained temperature was more accurate and within $\pm 0.1^\circ$ using the temperature unit of the Stellar spectrometer. The temperature at the top of the largest (ca 2 cm from the bottom of the tube) ice sample was generally about 2° higher than the temperature of the air/ N_2 flow measured by the spectrometer.

3. Relaxation theory

The observed 1H spin–lattice relaxation rate of water protons may be written in terms of a dipole–dipole interaction K_{tot}^{DD} (a sum of $K_{\text{intra}}^{DD}(r_{HH})$ and an intermolecular contribution $K_{\text{inter}}^{DD}(<r>)$). The latter is approximated in terms of the intramolecular contribution assuming the same correlation time. To a first approximation, using the BWR perturbation theory, the proton spin–lattice relaxation rate $R_1^{\text{exp}}(\omega, T)$ for ice can be expressed in terms of two equations [9]: The spin–lattice relaxation rate is given by,

$$R_1(\omega_0) = \frac{3}{10} K_{\text{tot}}^{DD} \tau_c [J_1(\omega_0) + 4J_2(2\omega_0)] \quad (1)$$

and the proton spin–spin relaxation rate is given by,

$$(1/T_2) \equiv R_2(\omega_0) = \frac{3}{20} K_{\text{tot}}^{DD} \tau_c \times (3J_0(0) + 5J_1(\omega_0) + 2J_2(2\omega_0)) \rightarrow \omega_0 \tau_c \gg 1 = \frac{9}{20} K_{\text{tot}}^{DD} \tau_c \times J_0(0). \quad (2)$$

The spectral densities of Equations (1) and (2) are defined as,

$$J_k(k\omega_0) = \int_0^\infty \langle D_{0k}^{2*}(\Omega_t) D_{0k}^2(\Omega_0) \rangle e^{-ik\omega t} dt \approx 5 \frac{\langle |D_{0k}^2(\Omega_0)|^2 \rangle}{1 + (k\omega_0 \tau_c)^2}. \quad (3)$$

where $D_{0k}^2(\Omega_0)$ is a Wigner rotation matrix element and a single-exponential decay of the correlation function is assumed [10] (see appendix). We combine Equations (1)–(3) to an expression for the water 1H spin–lattice NMRD

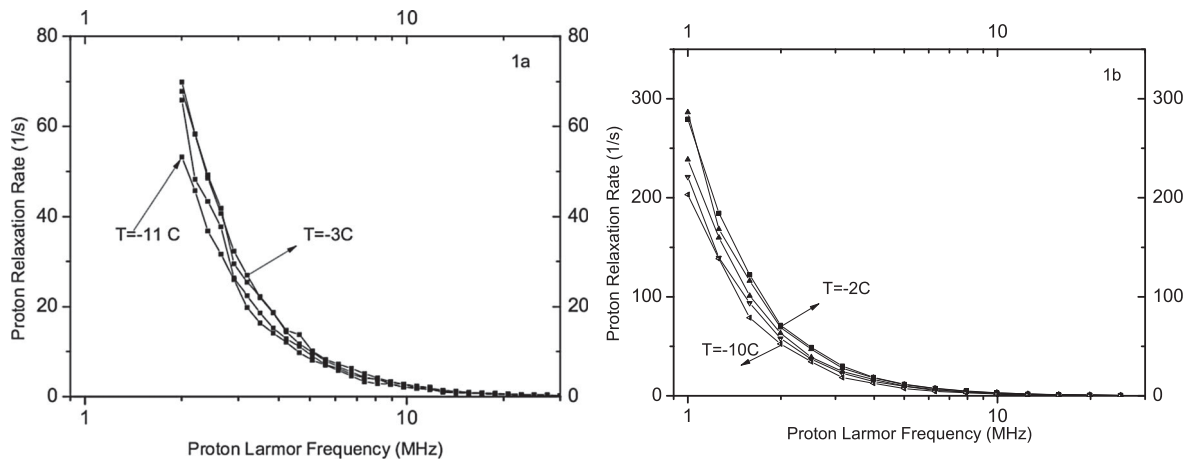


Figure 1. The Experimental measured proton T_1 NMRD profiles at temperatures -3°C , -5°C , -8°C and -11°C (1a, sample 2015) and -2°C , -3°C , -5°C , -7°C and -10°C (1b, sample 2017). The model parameters obtained from a non-linear least-square fit by Levenberg–Marquardt method using τ_c and $\langle T_2 \rangle$ as fitting parameters are shown in Table 1.

profile $R_1^{theory}(\omega_0)$,

$$R_1^{theory}(\omega_0) = \frac{2}{3T_2 \langle |D_{00}^2(\Omega)|^2 \rangle} \times \left[\frac{\langle |D_{01}^2(\Omega)|^2 \rangle + \langle |D_{02}^2(\Omega)|^2 \rangle}{\omega_0^2 \tau_c^2} \right]. \quad (4)$$

Equation (4) is the main equation of our approach and presuppose $\omega_0 \tau_c \gg 1$ and ignores angle-dependent relaxation. It is then used for two different dynamics models of water in hexagonal ice. Applied to the isotropic rotation diffusion model, the averaged Wigner matrix elements are all 1/5 and the result is a simple expression for the water proton T_1 NMRD profile of ice reading:

$$R_{1,diff}^{theory}(\omega_0) = \frac{4}{3} \left[\frac{1}{T_2 \tau_{c,diff}^2 \omega_0^2} \right]. \quad (5)$$

For the six-site exchange model (see [appendix](#)), the corresponding equation reads:

$$R_{1,exch}^{theory}(\omega_0) \approx \left[\frac{1}{T_2 \tau_{c,exch}^2 \omega_0^2} \right]. \quad (6)$$

From Equation (2) (see [appendix](#)), we obtain a relation between the two correlation times: $\tau_{c,exch} = 0.78 \tau_{c,diff}$. The analysis of the total dipole–dipole interaction $K_{tot}^{DD} = (K_{intra}^{DD}(r_{HH}) + K_{inter}^{DD}(< r >))$ is independent of dynamic model and from Equation (2) and the experimental $< T_2^{exp} >$ the ratio $K_{inter}^{DD}/K_{intra}^{DD}$ is given by

$$\frac{20}{9 \langle T_2^{exp} \rangle \tau_{c,diff}} / (3.659 \times 10^{10}) - 1 = \frac{K_{inter}^{DD}}{K_{intra}^{DD}(1.58)} \quad (7)$$

and for the six-site exchange model

$$\frac{1.279}{\langle T_2^{exp} \rangle \tau_{c,exch}} / (3.659 \times 10^{10}) - 1 = \frac{K_{inter}^{DD}}{K_{intra}^{DD}(1.58)} \quad (8)$$

4. Results

In Figure 1(left), the water proton spin–lattice relaxation NMRD profiles of hexagonal ice/snow (sample 2015) are displayed for proton Larmor frequencies ranging from 2 to 25 MHz and at four temperatures ($T = -3^\circ\text{C}$, -5°C , -8°C and -11°C). In Figure 1(right), the corresponding NMRD profiles are shown for sample 2017 where the proton Larmor frequencies are ranging from 1 to 20 MHz at temperatures $T = -2^\circ\text{C}$, -3°C , -5°C , -7°C and -10°C . The relaxation rate data show only the high-field wing of the $^1\text{H} - T_1$ NMRD profile. The spin–lattice relaxation rates at lower fields are too fast to be recorded. The experimental NMRD profiles are fitted to the theoretical NMRD profiles of Equations (5)

and (6) using only the correlation time as a fitting parameter. Thus, for a given $\langle T_2 \rangle$ value, the experimental proton T_1 -NMRD profiles were considered to be a function of τ_c , the proton Larmor frequency ω and temperature T . We derived the relation $\tau_{c,exch} = 0.78 \tau_{c,diff}$, however, it is not strictly confirmed in Table 1 but rather $\tau_{c,exch} \leq 0.85 \tau_{c,diff}$. It is understood as a consequence of the uncertainty of T_2 values. If the fitting instead uses both T_2 and τ_c as fitting parameters but with an initial value of $\langle T_2 \rangle$ within the error interval, the extracted parameter values are both within the uncertainty interval given in Table 1. The ratio (cf. Equation (6)) between K_{inter}^{DD} and K_{intra}^{DD} was about 0.4–0.8 (Table 1) and the intermolecular dipole–dipole contribution was between 28% and 44%. In [3], they estimate this ratio to 0.43 using a slightly larger proton–proton intra molecular distance of 1.62 Å. (this corresponds to 0.66 if $r = 1.58$ Å is used).

In [1] and [8], the relaxation rate Equation (1) was expressed in terms of the proton relaxation time T_1 and the effective correlation time τ_c , assuming $\omega_0 \tau_c \gg 1$.

$$T_1(T) = C(\omega_0) \times \tau_c(T). \quad (9)$$

where the numerical factor $C(\omega_0)$ is frequency dependent and for the diffusion model, it becomes

$$C_{diff}(\omega_0) = \frac{5}{3} \frac{\omega_0^2}{K_{real}^{DD}} \quad (10)$$

whereas for the six-site exchange model, it reads

$$C_{exch}(\omega_0) = \frac{1.79 \omega_0^2}{K_{real}^{DD}} \quad (11)$$

Lowe et al. [1] reported $C(10 \text{ MHz}) = 2.14 \times 10^5$ ($K_{real}^{DD} = 3.075 \times 10^{10}$), whereas Gran et al. [8] reported a value of $C(8 \text{ MHz}) = 4.74 \times 10^4$ ($K_{real}^{DD} = 8.884 \times 10^{10}$).

Table 1. The correlation times for the diffusion model $\tau_{c,diff}$ and in brackets [$\tau_{c,exch}$] for the six-site exchange model corresponding to fast motions in h-ice which are obtained by fitting the high-field NMRD profile $R_1^{exp}(\omega)$ given by Equations (5) and (6) to $R_1^{exp}(\omega, T)$ at temperatures ranging from -2°C to -10°C using a non-linear least-square fit by Levenberg–Marquardt method.

Snowflakes(T)	$[\tau_{c,exch}] \tau_{c,diff}$ (μs)	$K_{inter}^{DD}/K_{intra}^{DD}$	$< T_2^{exp} >$ (μs)	r_{HH} (Å)
$-3^\circ\text{C},*$	[2.8]3.7±0.5	0.4	12 ± 1	1.58
$-5^\circ\text{C},*$	[2.9]4.0±0.5	0.4–0.7	10.5 ± 1	1.58
lh $-5^\circ\text{C},*$	[3.0]3.9 ± 0.5	0.6	10 ± 1	1.58
$-8^\circ\text{C},*$	[3.3]4.3±0.5	0.8	9.4 ± 0.6	1.58
$-11^\circ\text{C},*$	[3.7] 4.8±0.5	0.7	7.4 ± 0.9	1.58
$-2^\circ\text{C},**$	[2.4]2.8±0.5	0.6	14.1 ± 1	1.58
$-3^\circ\text{C},**$	[2.6]3.5±0.5	0.7	12.8 ± 1	1.58
$-5^\circ\text{C},**$	[3.2]3.3 ± 0.5	0.6	10.2 ± 1	1.58
$-7^\circ\text{C},**$	[3.4]3.9±0.5	0.6	9.5 ± 0.6	1.58
$-10^\circ\text{C},**$	[4.3] 5.2±0.5	0.7	6.6 ± 0.9	1.58

Note: *Represents snow samples from 2015 and ** represent samples from 2017.

Table 2. A comparison with effective correlation times τ_c , from the literature.

Ice (T)	τ_c (μ s)	$\omega_0/2\pi$ (MHz)	Ref	How?
-3°C to -10°C	2.5–5.5	10	[1]	$T_{1p} = 2.14 \times 10^5 \tau_c$
-3°C to -10°C	1.8–3	50,55	[6]	$T_{1d} = 4.363 \times 10^5 \tau_c^f$
-3°C to -10°C	20–35	8	[8]	Equation (4)
-3°C to -10°C	2–5	37, 60	[11]	Figure 1
-3°C to -10°C	2.4–5.2	NMRD	This work	Table 1

Our values for both dynamic models fall in between these values. We have for the diffusion model (5.854–6.220) $\times 10^{10}$ and for the six-site exchange model (6.29–6.68) $\times 10^{10}$.

In Table 2, it is notable that the correlation times $\tau_{c,x}$ of the dipole–dipole interaction in our study are similar to previously published values except for Gran et al. [8] who report a considerably larger τ_c .

5. Conclusions

In this work, we demonstrated the use of fast field cycling measurements of $^1H - T_1$ NMRD profiles of water in hexagonal ice to extract the correlation time τ_c describing the water proton dipole–dipole correlation function. By considering this special case with considerable slow dynamics, short T_2 and relaxation in the $\omega_I \tau_c \gg 1$ regime the limited T_1 relaxation values at the high-field wing of a $^1H - T_1$ NMRD profile can be used to extract a good estimation of the effective dipole–dipole coupling constant K_{tot}^{DD} and the (shortest) correlation time responsible for the modulation of the proton dipole–dipole interaction. A basic assumption in the analysis is that the high-field wing is due to one single dispersion characterised by a single-exponential dipole–dipole correlation function. The spin–spin relaxation rate $\langle T_2^{\text{exp}}(T) \rangle$ can be determined for each temperature at one frequency (16.29 MHz) from the initial decay of the absolute value of the FID in the T_1 -NMRD experiment. The rather short T_2 ($\approx 10 \mu$ s) indicated that the contribution from inhomogeneous broadening is relatively small and could be neglected and that a spin-echo experiment was not possible. It should also be noticed that the BWR relaxation theory is a first approximation and may fail even though the conditions in this experiment are $T_1 \gg \tau_c$ and $T_2 \geq \tau_c$. Two dynamic models were used in the analysis, an isotropic rotation diffusion model and the more realistic six discrete site exchange model. It is clear that the approach cannot discriminate between the two dynamic models.

It was not possible to discriminate between snowflake h-ice and ordinary hexagonal ice using temperature-dependent $^1H - T_1$ measurements. However, the temperature is not uniform in the samples. If much higher

accuracy of the sample temperatures was possible, the activation energy may be determined.

Acknowledgments

Dr Tobias Sparrman is gratefully acknowledge for assistance with the NMRD spectrometer and for critically comments.

Disclosure statement

No potential conflict of interest was reported by the authors.

Funding

This work was financially supported by Swedish research council VR [grant no. D0437201]

ORCID

Per-Olof Westlund  <http://orcid.org/0000-0002-9277-4534>

References

- [1] D.E. Barnaal and I.J. Lowe, *J. Chem. Phys.* **48**, 4614 (1968).
- [2] J.D. Bernal and R.H. Fowler, *J. Chem. Phys.* **1**, 515 (1933).
- [3] L. Onsager and L.K. Runnels, *J. Chem. Phys.* **50**, 1089 (1969).
- [4] M. Weihaue, F. Noack and J. von Shutz, *Z. Physik* **246**, 91–96 (1971).
- [5] G.F. Bruno and M.M. Pintar, *J. Chem. Phys.* **58**, 5344 (1973).
- [6] B. Geil, T.M. Kirschgen and F. Fujara, *Phys. Rev. B* **72**, 014394 (2005).
- [7] W.R. Groes and C.M. Pennington, *Chem. Phys.* **315**, 1–7 (2005).
- [8] H-C. Gran, E.W. Hansen and B. Pedersen, *Acta Chem. Scand.* **51**, 24–30 (1997).
- [9] C.P. Slichter, *Principles of Magnetic Resonance, Springer Series in Solid-State Sciences* (Springer-Verlag, Berlin, 1990).
- [10] D.M. Brink and G.R. Satchler, *Angular Momentum* (Clarendon press, Oxford, 1993).
- [11] R. Blinc, H. Granicher, G. Lahajnar and I. Zupancic, *Z. Physik B* **22**, 211 (1975).
- [12] C.W. Gardiner, *Handbook of Stochastic Methods for Physics, Chemistry and Natural Sciences*, 2nd ed. (Springer, Berlin, 1985).

Appendix

A.1 The time-dependent proton spin dipole–dipole interaction due to exchange dynamics

The water protons are relaxed due to the motion of the intramolecular dipole–dipole interaction and can be described by the semi-classical dipole–dipole Hamiltonian:

$$H^{DD}(t) = \omega_D \sum_n \sum_m D_{0,m}^2(\theta(t), \phi(t)) D_{m,n}^2(\Omega_{ML}) T_n^2 \quad (\text{A1})$$

Here the dipole coupling constant is $\omega_D = -\sqrt{6}(\mu_0 \gamma_H^2 \hbar / 4\pi r_{HH}^3)$. We have introduced a molecular fixed frame of

ice which is oriented as described by the Wigner rotation matrix element having the Euler angles Ω_{ML} relative to the lab frame (L), where the latter is defined by the static magnetic field B_z along its z-axis. The time-dependent Euler angles $\alpha(t)$, $\beta(t)$ describe the orientation dynamics of the intra molecular proton vector r_{HH} motion relative to the ice crystal frame M. With this Hamiltonian, it is clear that one may expect angle-dependent spin relaxation. The second-rank spin tensor operator T_n^2 and the elements of the rank 2 Wigner Matrix are defined as [9, 10]:

$$T_0^2 = \frac{1}{\sqrt{6}}(I_{1,A}I_{-1,B} + I_{-1,A}I_{1,B} + 2I_{z,A}I_{z,B}) \quad (\text{A2})$$

$$T_{\pm 1} = \frac{1}{\sqrt{2}}[I_{\pm 1,A}I_{z,B} + I_{z,A}I_{\pm 1,B}] \quad (\text{A3})$$

$$T_{\pm 2} = I_{\pm 1,A}I_{\pm 1,B} \quad (\text{A4})$$

$$D_{0,0}^2(\theta(t)) = \frac{1}{2}(3 \cos^2(\theta(t)) - 1) \quad (\text{A5})$$

$$D_{0,\pm 1}^2(\theta(t), \phi(t)) = \mp \sqrt{\frac{3}{2}} \sin(\theta(t)) \cos(\theta(t)) e^{\mp i\phi(t)} \quad (\text{A6})$$

$$D_{0,\pm 2}^2(\theta(t), \phi(t)) = \sqrt{\frac{3}{8}} \sin^2(\theta(t)) e^{\mp i2\phi(t)} \quad (\text{A7})$$

A.2 A discrete six-site dynamics model

Instead of a rotational diffusion model, one may write down the expression for a spectral density using a discrete six-site chemical exchange model. In this model, one assume that water fulfills the rules of hydrogen bonds and jump between six different positions with the same probability. Water in hexagonal ice exchange between six different orientations are listed in Table A1. λ is the exchange rate for a water molecule moving from site I with orientation (θ_I, ϕ_I) to a vacancy at site k with orientation (θ_k, ϕ_k) , which is one of the other five orientations. The stochastic time modulation of the dipole-dipole interaction is described as a discrete jump processes between six different sites for bulk ice where the orientation of the intramolecular dipole-dipole interaction change.

A.2.1 The equation of motion

The master equation reads [12]

$$\frac{\partial}{\partial t} P(n, t|m, 0) = \sum_m W(n|m)P(n, t|m, 0) - W(m|n)P(n, t|m, 0) \quad (\text{A8})$$

where n and m denotes sites $1 \dots 6$. The transition rates $W(n|m) \equiv \lambda P(n, eq)$ which is the mean life time $1/\tau_m$ in site m and expressed in terms of the mean rate λ . For simplicity, we assume that the equilibrium populations of the different sites are the same and equal to $P(n, eq) = 1/6$. The exchange rate λ ,

is referring to the mean life time of each water orientations of the six sites. In the case of interface water, we have less than six different sites.

$$\frac{d}{dt} [P(n, t)] = [E][P(n, t)] \quad (\text{A9})$$

The discrete six-site model of a water molecule vacancy in the crystal and assuming that the change of water orientation in the crystal is described by the motion of this vacancy, which is filled up by any water orientation (1–6) in the vicinity of it. The master equation is reading:

$$\frac{d}{dt} \begin{bmatrix} P(\Omega_1, t|x, 0) \\ P(\Omega_2, t|x, 0) \\ P(\Omega_3, t|x, 0) \\ P(\Omega_4, t|x, 0) \\ P(\Omega_5, t|x, 0) \\ P(\Omega_6, t|x, 0) \end{bmatrix} = \begin{bmatrix} -5\lambda/6 & \lambda/6 & \lambda/6 & \lambda/6 & \lambda/6 & \lambda/6 \\ \lambda/6 & -5\lambda/6 & \lambda/6 & \lambda/6 & \lambda/6 & \lambda/6 \\ \lambda/6 & \lambda/6 & -5\lambda/6 & \lambda/6 & \lambda/6 & \lambda/6 \\ \lambda/6 & \lambda/6 & \lambda/6 & -5\lambda/6 & \lambda/6 & \lambda/6 \\ \lambda/6 & \lambda/6 & \lambda/6 & \lambda/6 & -5\lambda/6 & \lambda/6 \\ \lambda/6 & \lambda/6 & \lambda/6 & \lambda/6 & \lambda/6 & -5\lambda/6 \end{bmatrix} \times \begin{bmatrix} P(\Omega_1, t|x, 0) \\ P(\Omega_2, t|x, 0) \\ P(\Omega_3, t|x, 0) \\ P(\Omega_4, t|x, 0) \\ P(\Omega_5, t|x, 0) \\ P(\Omega_6, t|x, 0) \end{bmatrix}$$

This equation of motion is very symmetric and can be diagonalised by a product of Wang transformations which gives the solution using $\lambda = 1/\tau$:

$$\begin{bmatrix} P(\Omega_1, t|x, 0) \\ P(\Omega_2, t|x, 0) \\ P(\Omega_3, t|x, 0) \\ P(\Omega_4, t|x, 0) \\ P(\Omega_5, t|x, 0) \\ P(\Omega_6, t|x, 0) \end{bmatrix} = \begin{bmatrix} \frac{1}{6}(1 + 5e^{-t/\tau}) & \frac{1}{6}(1 - e^{-t/\tau}) & \frac{1}{6}(1 - e^{-t/\tau}) \\ \frac{1}{6}(1 - e^{-t/\tau}) & \frac{1}{6}(1 + 5e^{-t/\tau}) & \frac{1}{6}(1 - e^{-t/\tau}) \\ \frac{1}{6}(1 - e^{-t/\tau}) & \frac{1}{6}(1 - e^{-t/\tau}) & \frac{1}{6}(1 + 5e^{-t/\tau}) \\ \frac{1}{6}(1 - e^{-t/\tau}) & \frac{1}{6}(1 - e^{-t/\tau}) & \frac{1}{6}(1 - e^{-t/\tau}) \\ \frac{1}{6}(1 - e^{-t/\tau}) & \frac{1}{6}(1 - e^{-t/\tau}) & \frac{1}{6}(1 - e^{-t/\tau}) \\ \frac{1}{6}(1 - e^{-t/\tau}) & \frac{1}{6}(1 - e^{-t/\tau}) & \frac{1}{6}(1 - e^{-t/\tau}) \end{bmatrix}$$

Table A1. The functional values of the wigner functions for the six orientations of the proton proton vector

Ice (1–6)	θ	ϕ	$D_{0,0}^2(\theta(l))$	$D_{0,\pm 1}^2(\theta(l), \phi(l))$	$D_{0,\pm 2}^2(\theta(l), \phi(l))$
h1	35.25	180	0.50	0.577	$(-0.0833) * \sqrt{6}$
h2	35.25	-60	0.50	$(-0.1177 - 0.2041i) * \sqrt{6}$	$(0.04177 - 0.0720i) * \sqrt{6}$
h3	35.25	60	0.50	$(-0.2887 + 0.50i)$	$(0.0416 + 0.07213i) * \sqrt{6}$
h4	90	-30	-0.50	0.0	$(-0.125 - 0.2165i) * \sqrt{6}$
h5	90	-150	-0.50	0.0	$-0.125 + .2166i) * \sqrt{6}$
h6	90	90	-0.50	0.0	$(0.250) * \sqrt{6}$

$$\begin{aligned} & \begin{bmatrix} \frac{1}{6}(1 - e^{-t/\tau}) & \frac{1}{6}(1 - e^{-t/\tau}) & \frac{1}{6}(1 - e^{-t/\tau}) \\ \frac{1}{6}(1 - e^{-t/\tau}) & \frac{1}{6}(1 - e^{-t/\tau}) & \frac{1}{6}(1 - e^{-t/\tau}) \\ \frac{1}{6}(1 - e^{-t/\tau}) & \frac{1}{6}(1 - e^{-t/\tau}) & \frac{1}{6}(1 - e^{-t/\tau}) \\ \frac{1}{6}(1 + 5e^{-t/\tau}) & \frac{1}{6}(1 - e^{-t/\tau}) & \frac{1}{6}(1 - e^{-t/\tau}) \\ \frac{1}{6}(1 - e^{-t/\tau}) & \frac{1}{6}(1 + 5e^{-t/\tau}) & \frac{1}{6}(1 - e^{-t/\tau}) \\ \frac{1}{6}(1 - e^{-t/\tau}) & \frac{1}{6}(1 - e^{-t/\tau}) & \frac{1}{6}(1 + 5e^{-t/\tau}) \end{bmatrix} \\ & \times \begin{bmatrix} \delta\Omega_{1,x} \\ \delta\Omega_{2,x} \\ \delta\Omega_{3,x} \\ \delta\Omega_{4,x} \\ \delta\Omega_{5,x} \\ \delta\Omega_{6,x} \end{bmatrix} \frac{1}{6} \end{aligned} \quad (\text{A10})$$

where the stationary probabilities are the same for each site ($= 1/6$).

A.2.2 The dipole–dipole time correlation function

In NMR, the stationary dipole–dipole correlation function may be written as

$$\begin{aligned} & \langle D_{0,n}^{2,*}(\Omega(t))D_{0,n}^2(\Omega(0)) \rangle \\ & = \sum_i \sum_j D_{0,n}^{2,*}(\Omega_i)D_{0,n}^2(\Omega_j)P(\Omega_i, t|\Omega_j, 0)P_{eq}(\Omega_j) \end{aligned} \quad (\text{A11})$$

where the second-rank Wigner rotation matrix element $D_{0,n}(\Omega_I)$ is given in Equations (A6)–(A8). The correlation functions with $n = 0, 1, 2$ are single exponential using the conditional probabilities of Equation A10.

$$\begin{aligned} rhs & = \frac{1}{36} \left[\sum_{I=1}^6 \{5|D_{0,n}^2(\Omega_I)|^2 - \sum_{J \neq I} D_{0,n}^{2,*}(\Omega_I)D_{0,n}^2(\Omega_J)\} e^{-t/\tau} \right] \\ & + \langle D_{0,n}^2 \rangle^2 \end{aligned} \quad (\text{A12})$$

The average is an weighted sum over all possible values of the tensor function at the six sites.

$$\langle D_{0,n}^2 \rangle^2 = \frac{1}{36} \sum_{I,J=1}^6 D_{0,n}^{2,*}(\Omega_I)D_{0,n}^2(\Omega_J) \quad (\text{A13})$$

Evaluating the correlation functions, we obtain:

$$\langle D_{0,0}^{2,*}(\Omega(t))D_{0,0}^2(\Omega(0)) \rangle = 0.2557 \times e^{-(t/\tau)} - \langle D_{0,0} \rangle^2 \quad (\text{A14})$$

$$\langle D_{0,1}^{2,*}(\Omega(t))D_{0,1}^2(\Omega(0)) \rangle = 0.1667 \times e^{-(t/\tau)}, \quad \langle D_{0,1} \rangle = 0 \quad (\text{A15})$$

$$\langle D_{0,2}^{2,*}(\Omega(t))D_{0,2}^2(\Omega(0)) \rangle = 0.2083 \times e^{-(t/\tau)}, \quad \langle D_{0,2} \rangle = 0 \quad (\text{A16})$$

whereas the isotropic diffusion model give

$$\langle D_{0,n}^{2,*}(\Omega(t))D_{0,n}^2(\Omega(0)) \rangle = \frac{1}{5} \times e^{-(t/\tau_2)}, \quad \langle D_{0,n} \rangle = 0 \quad (\text{A17})$$

where $\tau_2 = 1/6D$.

A.2.3 Relaxation rate with discrete exchange spectral density function

Using Equations (A12) – (A17), then Equation (1) is slightly modified :

$$\begin{aligned} R_1(\omega_0) & = \frac{3}{2} R_{\text{real}}^{\text{max}}(0) \left[\frac{0.1667}{1 + \omega_0^2 \tau_{c,exch}^2} + 4 \frac{0.2083}{1 + 4\omega_0^2 \tau_{c,exch}^2} \right] \\ & \rightarrow \omega_0^2 \tau_{c,exch} \gg 1 \approx \frac{9}{16} \frac{K_{\text{real}}^{DD}(0)}{\omega_0^2 \tau_{c,exch}} \end{aligned} \quad (\text{A18})$$

And for the spin–spin relaxation rate:

$$\begin{aligned} R_2(\omega_0) & = \frac{3}{2} R_{\text{real}}^{\text{max}}(0) \left[\frac{3}{2} \times 0.25569 + \frac{5}{2} \frac{0.1667}{1 + \omega_0^2 \tau_{c,exch}^2} \right. \\ & \left. + \frac{0.2083}{1 + 4\omega_0^2 \tau_{c,exch}^2} \right] \rightarrow \omega_0^2 \tau_{c,exch} \gg 1 \approx 0.5753 K_{\text{real}}^{DD}(0) \tau_{c,exch} \end{aligned} \quad (\text{A19})$$

Which means that $R_1 = R_2$ in extreme narrowing and in the $\omega_I \tau_c \gg 1$ regime,

$$K^{DD} = \frac{1.738}{T_2 \tau_{c,exch}} \quad (\text{A20})$$

which gives

$$R_1(\omega_0) \rightarrow \omega_0 \tau_{c,exch} \gg 1 = \left[\frac{0.9776}{T_2 \omega_0^2 \tau_{c,exch}^2} \right] \quad (\text{A21})$$

A typical fitting of the theoretical relaxation dispersion data is displayed in Figure 1.

Consequently, the correlation time obtained for the rotation diffusion model should be multiplied with 0.8–0.9 to give the correlation time of the discrete exchange model. The latter correlation time is given in Table 1 within [. . .] brackets. A correlation time in μs also indicate that at low field the perturbation approach becomes questionable since the relaxation times are comparable with the correlation times τ_c .

A.3 Angle-dependent relaxation

If we consider Equation (A1) there is a coordinate system in the ice crystal where each water molecule reorients with respect to this coordinate system and if the reorientation motion is not isotropic there is a residual time-independent interaction thus shifting the resonance frequency. It is thus expected that the measured relaxation rate is an average of the angle-dependent relaxation rates. Experimentally, it has not been possible to detect angle-dependent proton relaxation in single water ice-crystals but without success [1].

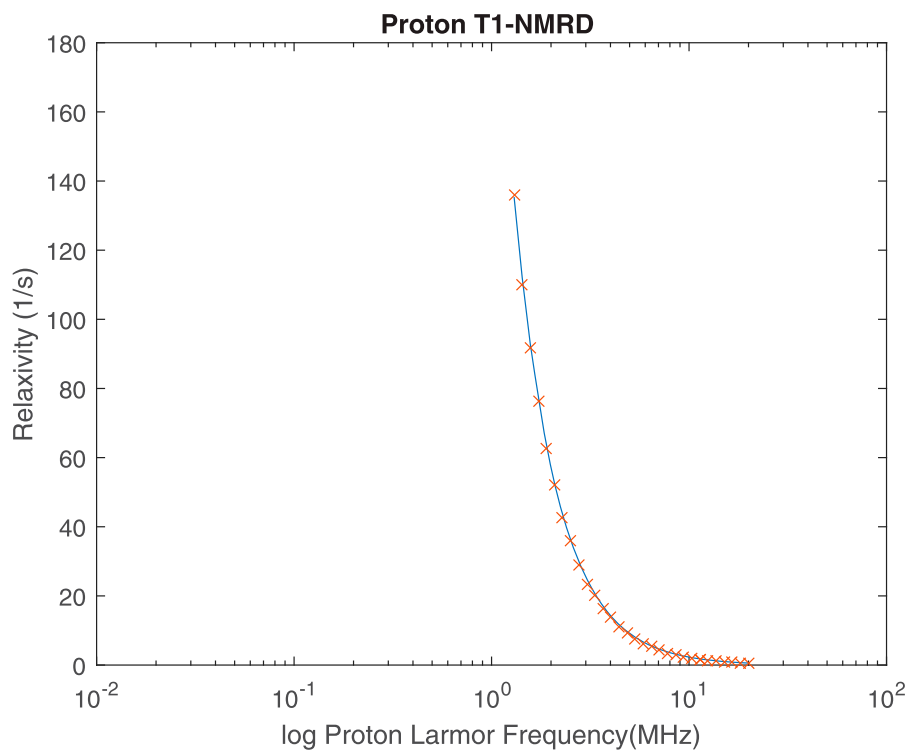


Figure A1. A typical fitting of the theoretical NMRD profile to the experimental measured proton T_1 NMRD profiles at temperature -5°C .